JOURNAL OF MATERIALS SCIENCE 27 (1992) 153–160

Mechanical alloying of Fe–B alloys

H. OKUMURA, K. N. ISHIHARA, P. H. SHINGU
Department of Metal Science and Technology, Kyoto University, Yoshida Sakyo-ku, Kyoto 606, Japan

H. S. PARK
Department of Metallurgical Engineering, Seoul National University, San 56-1 Shillim-2 dong Kwanak-gu, Seoul 151, Korea

S. NASU
Department of Metal Physics, Faculty of Engineering Science, Osaka University, Toyonaka, Osaka 560, Japan

Mechanical alloying (MA) of Fe–B alloy systems using a conventional ball mill has been performed. The structure change of $Fe_{100-x}B_x$ for the composition range $10 \leq x \leq 90$ has been investigated using X-ray diffractometry, thermal analysis, transmission electron microscopy, scanning electron microscopy and Mössbauer spectroscopy. According to the X-ray diffraction analysis, the sequences of transformation have been classified into three groups, $x \leq 20$, $25 \leq x \leq 35$ and $x \geq 50$ for $Fe_{100-x}B_x$. The amorphous phase whose composition is nearly $x = 30$, first appeared for the whole composition range. This amorphous phase changed into a tetragonal Fe_2B-like compound on further milling for 1000 h. On further milling of the $x = 50$ sample, the Fe_2B compound phase disappeared and orthorhombic FeB compound appeared.

1. Introduction

Recently, mechanical alloying (MA) has been proved to be effective in producing amorphous powders from elemental powder mixtures in a large number of alloy systems [1, 2]. There are many reports about the MA of transition metal (TM)–TM systems [3, 4], but few studies of TM–metalloid alloy systems have been performed. It is reported that amorphous phase formation in Fe–B systems using MA is rather difficult [5].

This paper describes the structure change induced by MA of elemental b c c iron and amorphous boron powders over a wide composition range. In order to perform atomic-level investigation of the phases produced, Mössbauer spectroscopy as well as the scanning electron microscopy was used for examination of macroscopic structures of the MA samples.

2. Experimental procedure

Elemental iron powder (purity 99%, several tens of micrometres in size) and amorphous boron powder (purity 97%, several micrometres in size) were used as starting materials. MA of the compositions $x = 10$, 15, 20, 25, 30, 35, 50, 60, 70, 80 and 90 for $Fe_{100-x}B_x$ was performed. The MA process was carried out for up to 1000 h using a stainless steel pot (height 16 cm, i.d. 13 cm) and balls (diameter 0.9 cm), under an argon atmosphere. The total weight of balls was 4 kg and the weight ratio of balls to powder was 100. The rotation rate of the pot was 90 r.p.m.

After processing, small quantities of powder were removed in a grove box filled with argon. The structure was examined by X-ray powder diffractometry (XRD) using CuK_α radiation with graphite monochromator. The thermal stability was investigated by differential scanning calorimetry (DSC) at a heating rate of 20 K min^{-1} from room temperature to 873 K under an argon flow atmosphere. The microscopic structure was investigated using a Mössbauer spectroscope with γ-rays radiated from a ^{57}Co.

The mechanical grinding (MG) of FeB intermetallic compound was also performed under the same experimental conditions as MA.

3. Results

3.1. Macroscopic structure

The macroscopic alloying process of $Fe_{80}B_{20}$ samples in the initial stages was investigated by SEM with electron probe microanalysis (EPMA). The images with secondary electrons and BK_α X-ray emission are shown in Fig. 1. After a MA time of 1 h (a), most of the boron powders were outside the iron powder particles, while the iron particles were flattened by ball milling. After 2 h milling (b), flattened boron particles were observed, and they were somewhat taken into iron particles. After 4 h milling (c), many flaky and needle-like iron particles were observed, and the lamellar structure can be seen in the high magnification photograph. Boron particles began to become embedded in the iron matrix due to kneading by the iron particles. After 7 h milling (d), the needle-shaped iron particles lost their sharpness and became roundish. A homogeneous dispersion of boron was achieved in the cold-welded iron particles.

0022–2461/92 $03.00 + .12

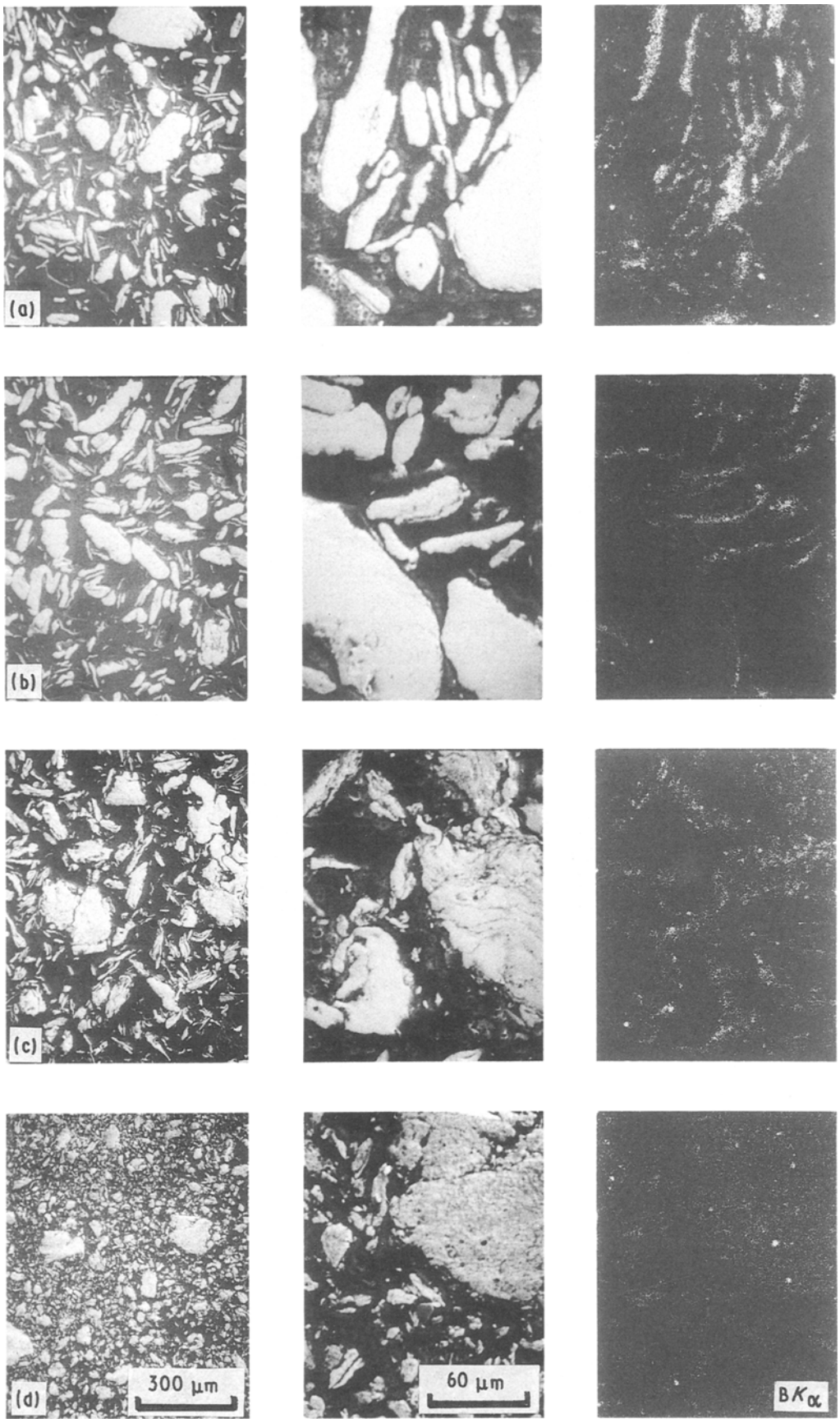

Figure 1 SEM images of $Fe_{80}B_{20}$ samples ball milled for (a) 1 h, (b) 2 h, (c) 4 h and (d) 7 h.

This milling process is similar to that of ductile transition metal (TM)–TM systems.

3.2. Structure examination by X-ray analysis

After a short milling time, the amorphous phase partially appeared for the whole composition range. The amorphous phase was confirmed by the use of Mössbauer spectroscopy (see later). After further milling, the sequences of structure change could be classified into three groups according to the XRD

patterns: (A) x = 10, 15, 20; (B) x = 25, 30, 35; (C) x = 50, 60, 70, 80, 90, for $Fe_{100-x}B_x$.

3.2.1. Group A: $Fe_{80}B_{20}$

XRD patterns of the $Fe_{80}B_{20}$ sample for various milling times are shown in Fig. 2. No compound phase appeared even after MA of 1000 h. Successive broadening of bcc iron peaks were observed, especially on the high-angle side, and an almost steady state was attained at an MA time of 140 h. Using Scheller's method, we found that the size of the iron crystalline particle estimated from the (1 1 0) diffraction peak was about 6 nm at MA 140 h, and did not change appreciably for longer MA times.

3.2.2. Group B: $Fe_{70}B_{30}$

XRD patterns of the $Fe_{70}B_{30}$ sample for various milling times and of the sample heated to 873 K after MA 1000 h are shown in Fig. 3a. Broadening of the bcc Fe peaks was observed up to MA of 700 h. A compound phase appeared by MA of 1000 h. By heating up to 873 K, both the compound peaks and the bcc Fe peaks were sharpened. This compound was quite similar to t-Fe_2B (tetragonal) [6]. The calculated diffraction pattern of t-Fe_2B is shown in Fig. 3b. In the pattern of the compound obtained by the MA method, there is no (2 0 0) plane peak, which should exist if the compound is t-Fe_2B. Therefore, the atomic structure of this compound should be different from that of t-Fe_2B. This compound is designated x-Fe_2B in this paper.

3.2.3. Group C: $Fe_{50}B_{50}$

XRD patterns of the $Fe_{50}B_{50}$ samples for various milling times are shown in Fig. 4.

The compound x-Fe_2B phase was deduced to appear at MA 380 h, because this XRD pattern was similar to that of $Fe_{70}B_{30}$ ball milled for 1000 h. Further milling changed this compound to FeB (orthorhombic), and single FeB phase was obtained at MA 1000 h.

For $Fe_{20}B_{80}$ and $Fe_{10}B_{90}$ samples, homogeneity was not achieved even after MA of 1000 h.

In summary, the major changes in each group were:
(A) Fe + B → amorphous + Fe
(B) Fe + B → amorphous + Fe → Fe_2B
(C) Fe + B → amorphous + Fe → Fe_2B → FeB

In the following sections, the detailed results of samples for three compositions x = 20, 30 and 50 belonging to groups A, B and C, respectively, are described.

3.3. Group A

DSC thermograms of the $Fe_{80}B_{20}$ sample are shown in Fig. 5. The area of an exothermic peak is saturated at MA 140 h and the value was about 120 $J\,g^{-1}$. The exothermic peak at about 760 K corresponds to the crystallization of amorphous phase into bcc Fe and

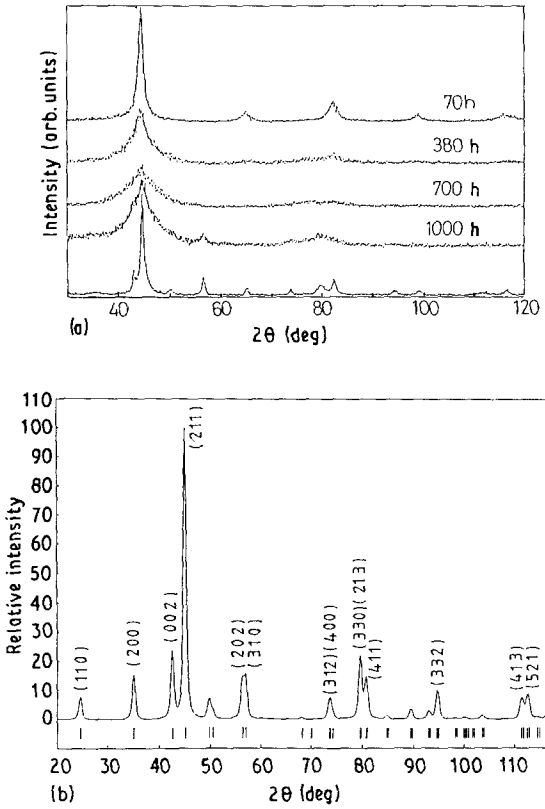

Figure 3 (a) XRD patterns of $Fe_{70}B_{30}$ samples ball milled for various times and of the sample heated up to 873 K after MA for 1000 h. (b) Calculated XRD pattern of t-Fe_2B.

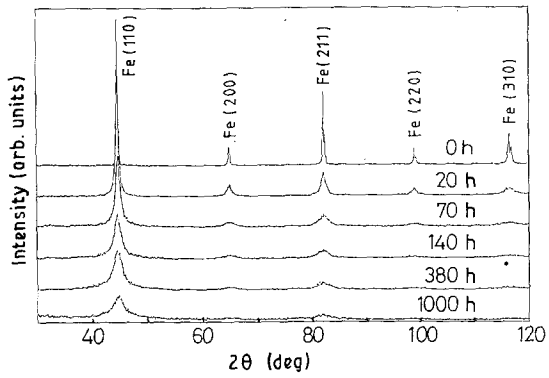

Figure 2 XRD patterns of $Fe_{80}B_{20}$ samples ball milled for various times.

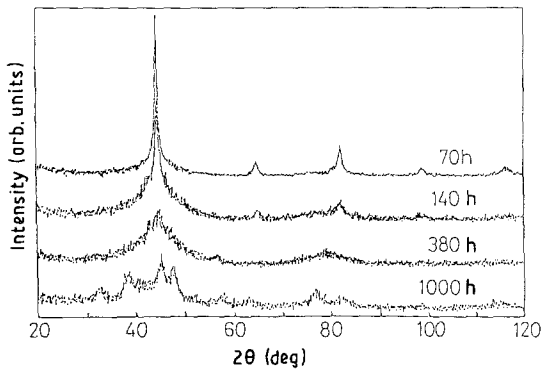

Figure 4 XRD patterns of $Fe_{50}B_{50}$ samples ball milled for various times.

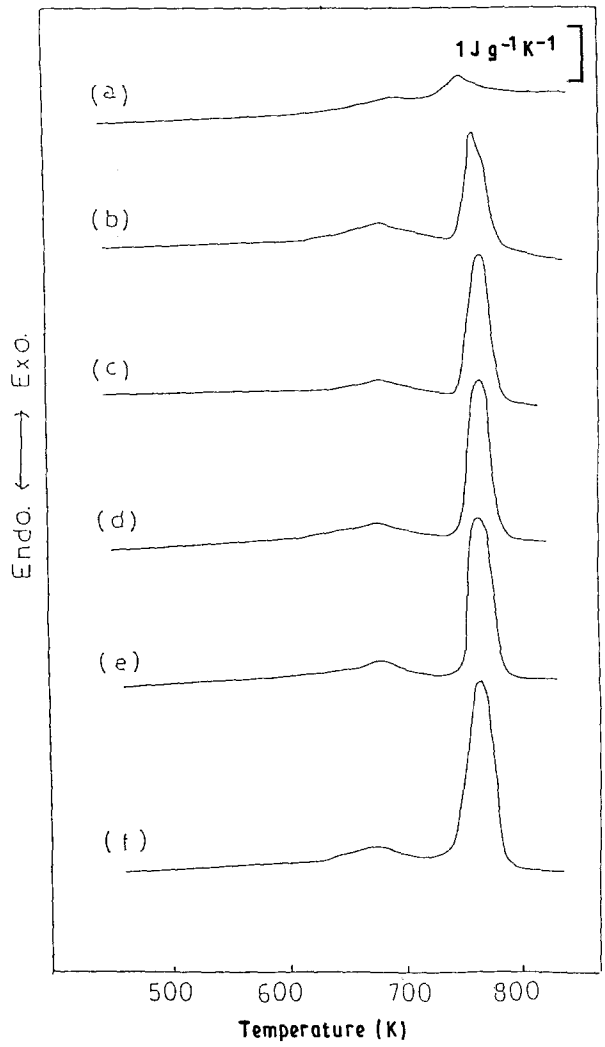

Figure 5 DSC thermograms of $Fe_{80}B_{20}$ samples ball milled for (a) 20 h, (b) 140 h, (c) 380 h, (d) 500 h, (e) 700 h, (f) 1000 h.

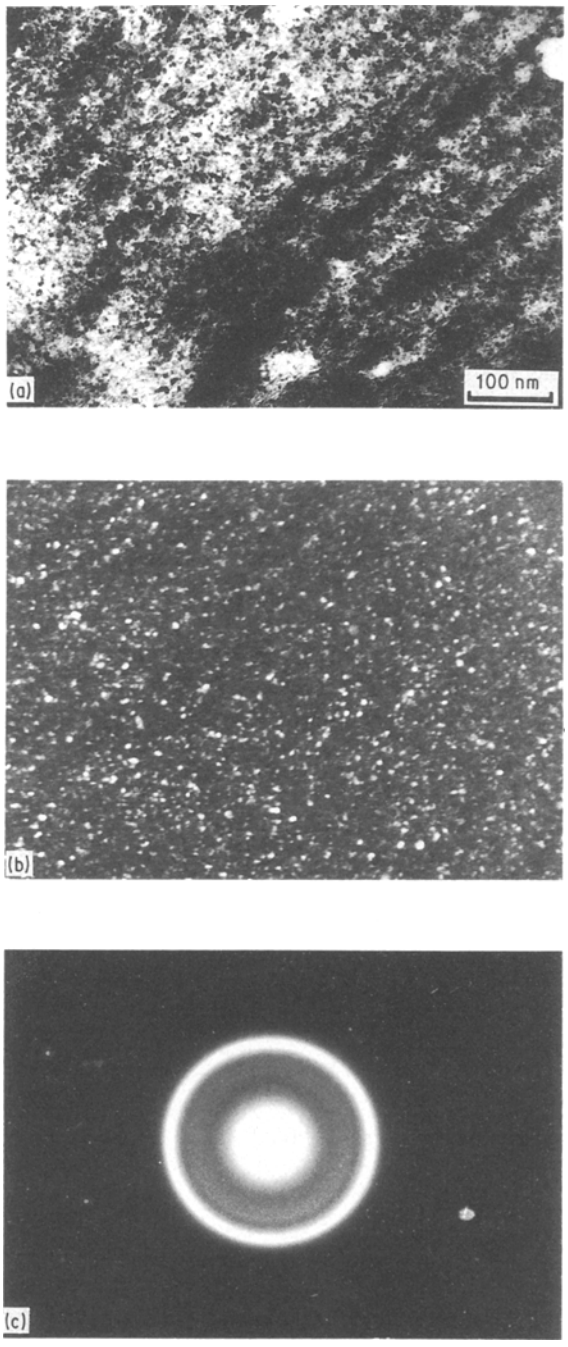

Figure 6 Transmission electron micrographs of (a) bright-field image, (b) dark-field image and (c) electron diffraction pattern of $Fe_{80}B_{20}$ sample ball milled for 1000 h. The dark-field image is taken from the strongest diffraction ring.

x-Fe_2B compound, which was confirmed by X-ray analysis.

Fig. 6 shows TEM images of the $Fe_{80}B_{20}$ sample ball milled for 1000 h. The bcc Fe particles, of nanometre order, can be observed both in bright-field (a) and dark-field (b) images.

In order to investigate the structure at the atomic level, Mössbauer spectroscopy of the $Fe_{80}B_{20}$ sample was performed. Broad components between six spectra of the bcc Fe absorbed line for the MA 140 h samples were found, as shown in Fig. 7b. These new absorption lines became clearer after MA of 1000 h (Fig. 7c), although the spectra of bcc Fe remained clearly visible. These broad spectra matched well those of rapidly quenched $Fe_{80}B_{20}$ amorphous ribbon in Fig. 7d. Hence it was concluded that the bcc Fe and amorphous phase co-existed in the MA powder.

3.4. Group B

DSC thermograms of the $Fe_{70}B_{30}$ sample are shown in Fig. 8. The amount of exothermic heat is saturated at MA 140 h at a value of $\sim 240\,J\,g^{-1}$. The sharp exothermic peak shifted from 760 K at MA 140 h to 738 K at MA 700 h, and disappeared at MA 1000 h when another broad peak appeared. The decrease in exothermal heat and the change of peak shape were attributed to the formation of the compound x-Fe_2B during MA, which was confirmed by X-ray analysis, as shown in Fig. 3a. After heating to 873 K, all the MA samples changed to the mixed phase of bcc Fe and compound x-Fe_2B, again confirmed by X-ray analysis.

Fig. 9 shows TEM images of the $Fe_{70}B_{30}$ sample ball milled for 700 h. The amorphous matrix phase, including some bcc Fe particles of nanometre size, can be observed both in bright-field (a) and dark-field (b) images.

The Mössbauer spectra of the $Fe_{70}B_{30}$ sample showed that the six broad ferromagnetic spectra which have internal magnetic fields smaller than the

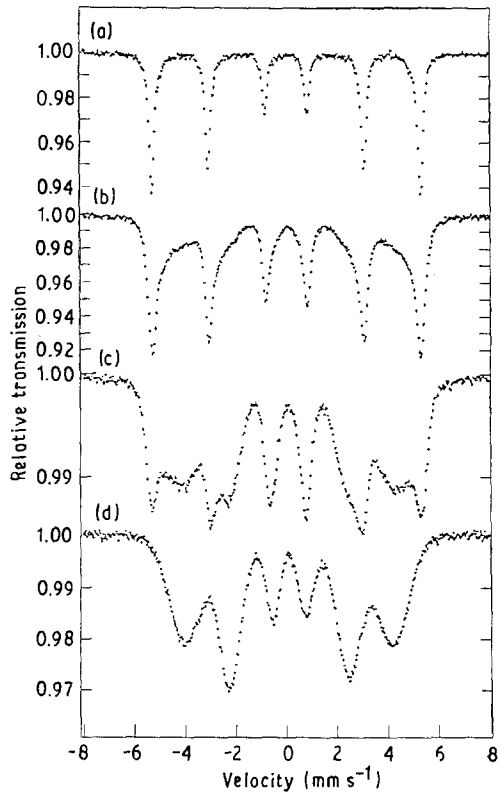

Figure 7 Mössbauer spectra of $Fe_{80}B_{20}$ samples: (a) iron; (b) MA 140 h; (c) MA 1000 h; (d) amorphous ribbon.

bcc Fe, increased with milling time, as shown in Fig. 10. These spectra are, as mentioned in the previous section, due to the amorphous phase. At a MA time of 700 h (c), almost single amorphous phase was obtained, but after a MA time of 1000 h (d), the spectra were slightly sharpened and shifted internally, and the ratio of intensity also changed. These spectra were similar to those of the $Fe_{65}B_{35}$ MA 1000 h sample (f), which was the single phase of x-Fe_2B compound. This change is consistent with both X-ray analysis and DSC analysis.

3.5. Group C

DSC thermograms of the $Fe_{50}B_{50}$ sample are shown in Fig. 11. As the fraction of compound increased, the amount of exothermic heat decreased. Only a small exothermic peak remained after MA of 700 h. After heating to 873 K, compounds x-Fe_2B and FeB were obtained at MA 140 h and single FeB phase was obtained after MA of 380 h, as confirmed by X-ray analysis.

Fig. 12 shows the results of Mössbauer spectroscopy of the samples (a) α-Fe, (b) $Fe_{50}B_{50}$ MA 1000 h, (c) FeB compound and (d) $Fe_{50}B_{50}$ MG 1000 h. The six spectra of bcc Fe had clearly disappeared after MA for 1000 h (b). The shape and positions of absorbed spectra in this sample were very similar to those of FeB compound (c).

In the case of mechanical grinding (MG) of the FeB intermetallic compound, no observable change of the XRD pattern was detected and only broadening of FeB peaks was noted. In the thermograms of these samples, a small exothermic peak appeared at about

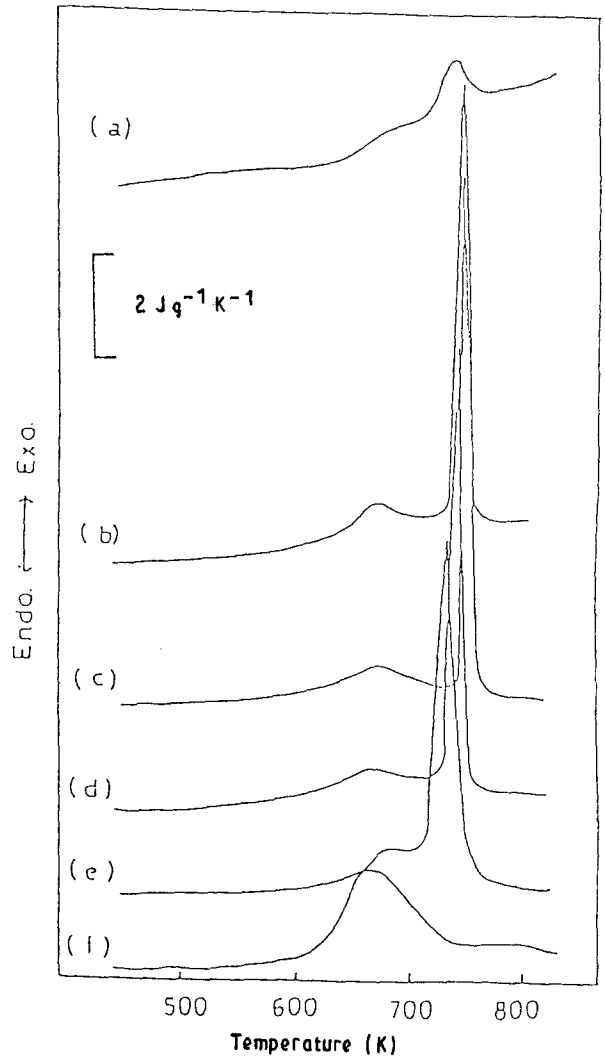

Figure 8 DSC thermograms of $Fe_{70}B_{30}$ samples ball milled for (a) 20 h, (b) 140 h, (c) 380 h, (d) 500 h, (e) 700 h, (f) 1000 h.

765 K for the sample MG for 20 h and did not change appreciably until MG for 1000 h. The Mössbauer spectra of the sample MG for 1000 h are shown in Fig. 12d. These spectra are similar to those of the $Fe_{50}B_{50}$ sample MA for 1000 h (b).

Consequently, compound FeB phase was very stable and was not changed to the other phases by MG. This FeB could also be obtained by MA of elemental iron and boron powders.

4. Discussion

Mechanical alloying can be done with iron, and boron which is a non-ductile element. However, it takes a longer time to alloy to a uniform composition compared with the MA time for the ductile metals. Therefore, regardless of the composition of the MA powders, alloying of the low boron concentration side is obtained initially. Then, the alloying concentration of the MA samples gradually changes to the initial concentration. For $Fe_{20}B_{80}$ and $Fe_{10}B_{90}$ samples, homogeneity was not obtained even after MA for 1000 h.

The heat of mixing in the Fe–B alloy system is about -32 kJ mol^{-1} at 298 K [7] and this can be a sufficient value to produce the amorphous phase. This

is clearly one factor influencing amorphous phase production using solid state reaction by MA. However, it is difficult to obtain atomic order homogeneity of iron and boron because of the hardness and brittleness of boron. In this system, the formation of an amorphous phase by liquid quenching has been reported in the composition range $11 \leq x \leq 35$ for $Fe_{100-x}B_x$ [8], while by using the r.f.-sputtering method, amorphous alloys have been fabricated in the wider chemical composition range $10 \leq x \leq 90$ [9]. However, in the present MA experiments, the amorphous forming ability is limited to the narrow composition range near $x = 30$. It is reported by Nakajima *et al.* [8] that in rapid quenching, the higher the boron concentration, the higher the crystallization temperature becomes. This means that the thermal stability of the amorphous phase increases with increasing boron concentration. This is the reason why the amorphous phase of the composition near $x = 30$ has only been produced by MA.

As previously reported in the MA of Al–Fe systems [10], the Mössbauer effect is a very useful means to examine the MA process, especially the formation of amorphous phase. In the present experiment, the existence of the amorphous phase was confirmed using Mössbauer spectroscopy by comparison of the data with those for rapidly quenched ribbon.

In Table I, the crystallization temperature, activation energy of crystallization and exothermic heat of

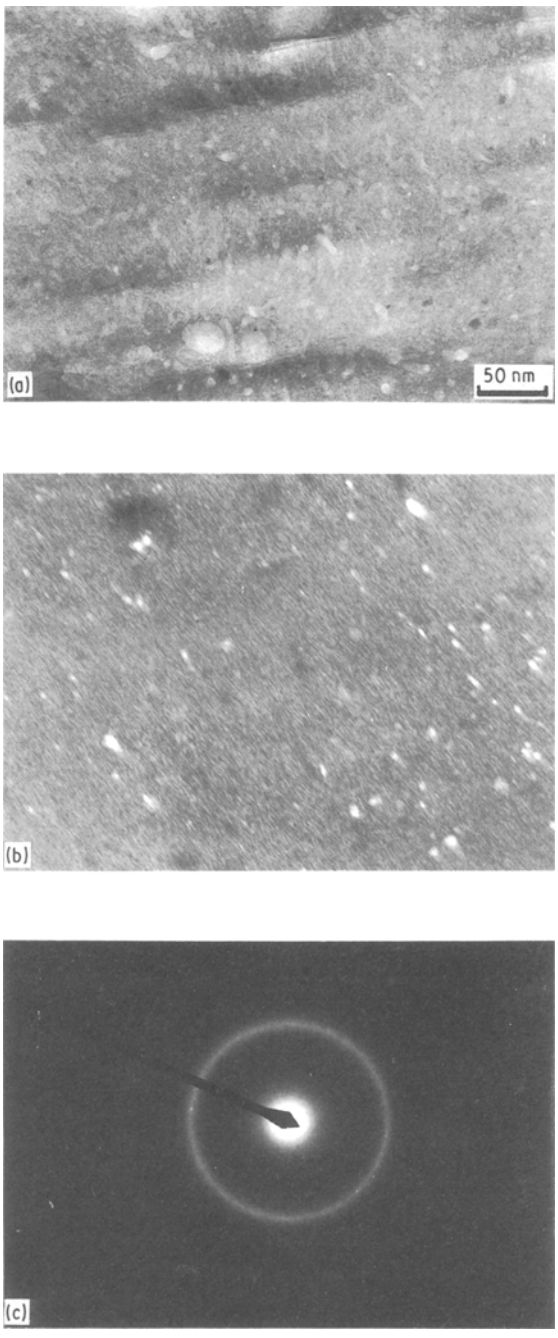

Figure 9 Transmission electron micrographs of (a) bright-field image, (b) dark-field image and (c) electron diffraction pattern of $Fe_{70}B_{30}$ sample ball milled for 700 h. The dark-field image is taken from the strongest diffraction ring.

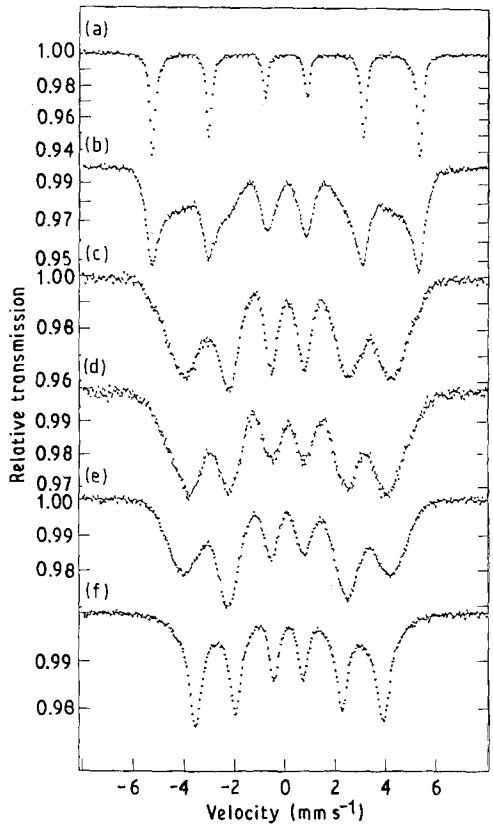

Figure 10 Mössbauer spectra of $Fe_{70}B_{30}$ samples: (a) iron; (b–d) $Fe_{70}B_{30}$, (b) MA 140 h (c) MA 700 h, (d) MA 1000 h; (e) $Fe_{80}B_{20}$ amorphous ribbon, (f) $Fe_{65}B_{35}$ MA 1000 h.

TABLE I Crystallization temperature, activation energy and exothermic heat of MA amorphous and rapidly quenched amorphous phases

Sample	Crystallization temperature (K)	Activation energy ($kJ\,mol^{-1}$)	Exothermic heat ($J\,g^{-1}$)
$Fe_{70}B_{30}$ MA 700 h	738	240	240
$Fe_{80}B_{20}$ RQ ribbon	738	200	185

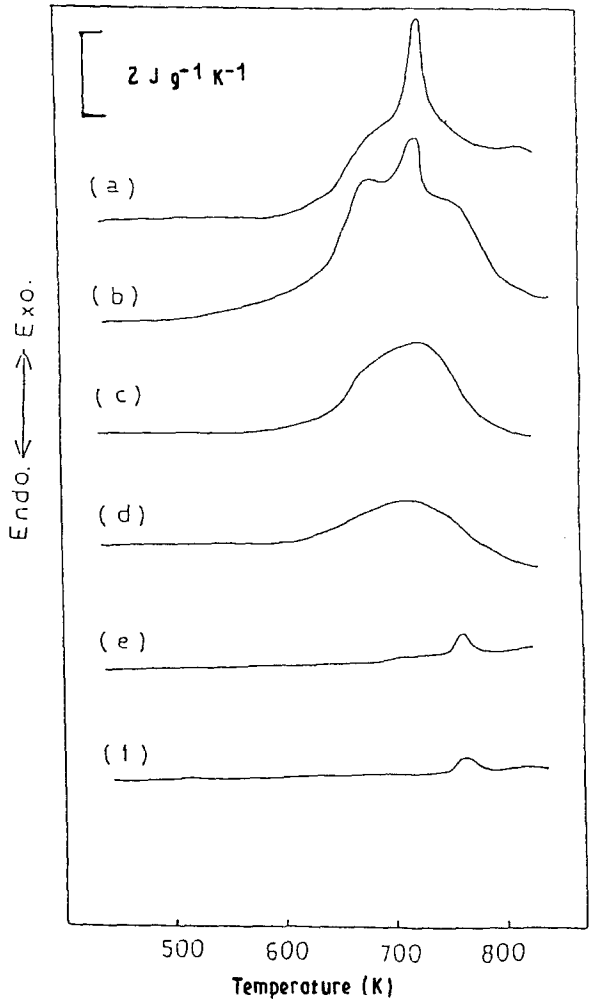

Figure 11 DSC thermograms of $Fe_{50}B_{50}$ samples ball milled for (a) 20 h, (b) 140 h, (c) 380 h, (d) 500 h, (e) 700 h, (f) 1000 h.

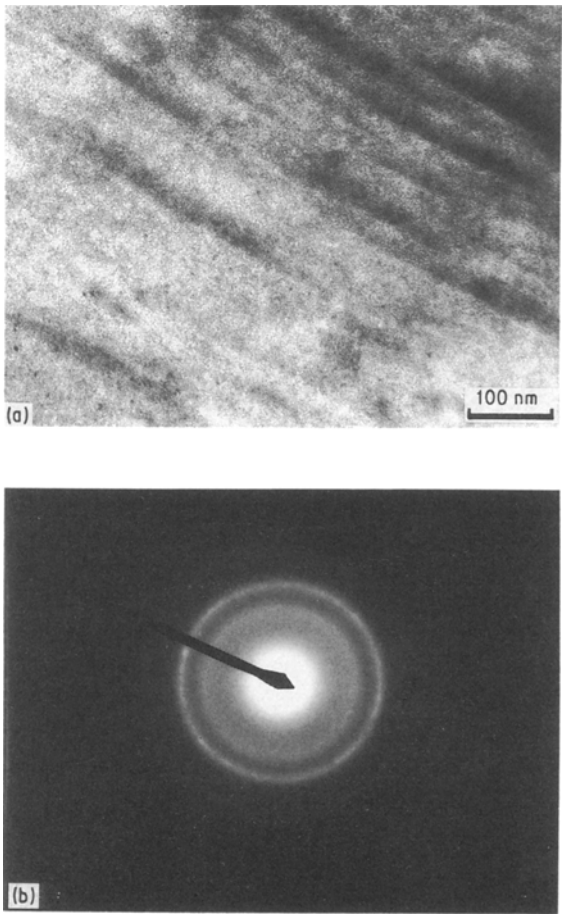

Figure 13 TEM images and electron diffraction pattern of $Fe_{78}Si_9B_{13}$ samples ball milled for 1000 h: (a) bright-field image; (b) electron diffraction pattern.

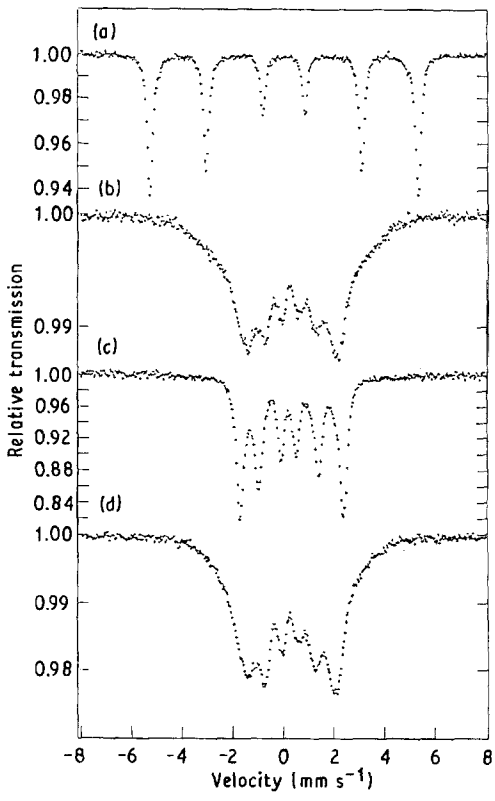

Figure 12 Mössbauer spectra of $Fe_{50}B_{50}$ samples: (a) iron; (b) MA 1000 h; (c) compound; (d) MG 1000 h.

amorphous phases obtained by MA and rapid quenching are listed. The crystallization temperatures of both samples are identical. From the Kissinger plot [11], the amorphous phase produced by MA has somewhat larger activation energy of 240 kJ mol^{-1} than that of the rapidly quenched amorphous phase [12]. The reason for the slightly higher value of crystallization heat for the MA sample is due to the reaction of iron and boron which has changed directly into the compound.

In order to investigate the influence on the MA of Fe–B binary system of the addition of a third element, MA of the sample with iron, boron and silicon was performed up to 1000 h. Fig. 13 shows transmission electron micrographs of the $Fe_{78}Si_9B_{13}$ MA 1000 h sample. A more homogeneous amorphous phase was obtained compared with the amorphous phase of the $Fe_{70}B_{30}$ MA 700 h sample, shown in Fig. 9. Thus, the amorphous phase is more easily formed by adding silicon to the Fe–B binary system.

An energy-dispersive X-ray chemical analysis was employed to investigate the contamination of MA samples. The contamination with nickel and chromium from the stainless steel pot and balls was at most 2 wt % of the MA sample after 1000 h milling. It is thought that amorphization using the MA method is not essentially related to the contamination from the pot and balls.

5. Conclusions

1. Iron and metalloid boron can be alloyed by mechanical alloying.

2. An amorphous phase near the composition of $Fe_{70}B_{30}$ has been obtained by the MA method.

3. For higher boron concentration samples, the formation of compounds of iron and boron occurs after ball milling for a long time.

References

1. C. POLITIS and W. L. JOHNSON, *J. Appl. Phys. Lett.* **60** (1986) 1147.
2. R. B. SCHWARZ and C. C. KOCH, *Appl. Phys. Lett.* **49** (1986) 146.
3. R. B. SCHWARZ and W. L. JOHNSON, *Phys. Rev. Lett.* **51** (1983) 415.
4. E. HELLSTERN and L. SCHULTZ, *Z. Phys. Chem.* **157** (1988) 215.
5. L. SCHULTZ and E. HELLSTERN, *ibid.* **157** (1988) 203.
6. P. VILLARS and L. D. CALVERT, "Pearson's Handbook of Crystallographic Data for Intermetallic Phases", Vol. 2 (American Society for Metals, Metals Park, OH, 1985) p. 1297.
7. Y. O. ESIN, V. M. BAEV, M. S. PETRUSHEVSKIY and P. V. GELD, *Izv. Akad. Nauk SSSR Met.* **4** (1975) 82.
8. T. NAKAJIMA, I. NAGAMI and H. INO, *J. Mater. Sci. Lett.* **5** (1986) 60.
9. W. HOVING, F. van der WOUDE, K. H. J. BUSCHOW and I. VINCZE, *J. Non-Cryst. Solids* **61/62** (1984) 421.
10. P. H. SHINGU, B. HUANG, S. R. NISHITANI and S. NASU, *Suppl. Trans. JIM* **29** (1988) 3.
11. H. E. KISSINGER, *Analyt. Chem.* **29** (1957) 1702.
12. F. E. LUBORSKY, *Mater. Sci. Engng* **28** (1977) 139.

Received 13 August 1990
and accepted 12 February 1991